Thermal effects on yielding and wetting-induced collapse of recompacted and intact loess

Authors: C. W. W. Ng, Q. Cheng* and C. Zhou

*Corresponding author

Information of the authors

Prof. C. W. W. Ng

CLP Holdings Professor of Sustainability, Department of Civil and Environmental Engineering, Hong Kong University of Science and Technology, Clear Water Bay, Kowloon, Hong Kong.

E-mail: cecwwng@ust.hk

Dr Q. Cheng

Doctor, Department of Civil and Environmental Engineering, Hong Kong University of Science and Technology, Clear Water Bay, Kowloon, Hong Kong.

E-mail: qcheng@ust.hk

Dr C. Zhou

Research Assistant Professor, Department of Civil and Environmental Engineering, Hong Kong University of Science and Technology, Clear Water Bay, Kowloon, Hong Kong.

E-mail: czhou@connect.ust.hk

ABSTRACT

Yielding and wetting-induced collapse are two important interrelated aspects of unsaturated loess behaviour. Previous studies on loess are generally under a single temperature condition. The principal objective of this study is to investigate thermal effects on yielding and wetting-induced collapse of recompacted and intact loess. Isotropic compression tests were carried out to determine yield stress at different suctions (0 and 100 kPa) and temperatures (5, 23 and 50°C). Moreover, wetting tests were conducted at various temperatures and stresses. The results of wetting tests were interpreted using the measured yield stress at various suctions and temperatures. It is found that yield stress decreases with decreasing suction (wetting-induced softening). The wetting-induced softening of recompacted loess is more significant at a higher temperature. The observed thermal effects on wetting-induced softening are likely because with decreasing suction, the stabilizing inter-particle normal force decreases more at a higher temperature. On the other hand, when the applied stress reaches the yield stress during wetting, yielding and plastic volumetric contraction can be observed. More importantly, wetting-induced contraction of recompacted loess at 50°C is about three times of that at 5°C. The larger contraction at 50°C is mainly because the wetting-induced softening is larger at a higher temperature.

Keywords: temperature; yielding; wetting; collapse; recompacted and intact loess

INTRODUCTION

Unsaturated loess has a metastable structure, which can be maintained temporarily by suction (Ng et al., 2016c). During wetting process, the metastable structure may be destroyed, leading to volumetric collapse of loess. The wetting-induced collapse may induce excessive ground movements and serious damages to geotechnical structures (Gens, 2010). According to elasto-plastic theory for unsaturated soil (e.g., Alonso et al., 1990), wetting-induced collapse is closely related to the yielding behaviour. Hence, it is of great importance to fully understand the yielding behaviour and wetting-induced collapse of unsaturated loess.

Many efforts have been made to investigate the yielding behaviour of unsaturated soil (Wheeler and Sivakumar, 1995; Cui and Delage, 1996; Villar, 1999; Lloret et al., 2003). A major conclusion from these previous studies is that the yield stress of unsaturated soil decreases with decreasing suction (wetting-induced softening). At a given suction, some researchers found that the yield stress decreases with increasing temperature (thermal induced softening) (Cekerevac and Laloui, 2004; Tang et al., 2008; Di Donna and Laloui, 2015). As far as the authors are aware, however, previous researches seldom compared the degree of wetting-induced softening at various temperatures. Furthermore, the difference between wetting-induced softening of recompacted and intact specimens is not clear.

As far as wetting-induced collapse is concerned, most previous studies focused on stress effects (Lawton et al., 1989, Pereire and Fredlund, 2000; Sun et al., 2007; Munoz-Castelblanco et al., 2011; Vilar and Rodrifues, 2011, Jiang et al., 2012). It is found that the maximum collapse occurs when the mean net stress equals to the

initial yield stress of unsaturated soil. Although thermal effects on soil behaviour are well recognized (Campanella and Mitchell, 1968; Abuel-Naga et al., 2007; Uchaipichat and Khalili, 2009; Zhou et al., 2015a; Ng et al., 2016a), as far as the authors are aware, only two studies have been reported to investigate thermal effects on wetting-induced collapse (Romero et al., 2003; Haghighi et al., 2011). Romero et al. (2003) found that, for recompacted loose Boom clay, wetting-induced volumetric strains measured at 22 and 80℃ are almost the same. Haghighi et al. (2011) found that the collapse volumetric strain of recompacted Kaolin clay at 20℃ is slightly larger than that at 50℃ and the maximum difference is about 4%. It should be noted that suction and temperature dependent yield stresses are not reported in the above two studies. Consequently, the observed thermal effects on soil collapse cannot be properly interpreted and fully understood within elastoplastic framework. Moreover, wetting-induced collapses of intact and recompacted loess were not compared by previous researchers. The difference between wetting-induced collapse of recompacted and intact loess specimens is not clear.

In this study, a series of isotropic compression tests were conducted on recompacted and intact loess specimens at different suctions (0 and 100 kPa) and temperatures (5, 23 and 50℃). Moreover, a series of wetting tests were carried out on recompacted and intact loess specimens at different confining stresses (50 and 110 kPa) and temperatures (5, 23 and 50℃). The results of wetting tests were analysed using the measured yield stress.

TEST PROGRAMME

The principal objective of this study is to investigate thermal effects on yielding and wetting-induced collapse of recompacted and intact loess. To achieve this objective, two series of suction and temperature controlled isotropic tests were conducted. In the first series, eight compression tests were carried out to determine suction and temperature dependent yield stress and yielding behaviour. Three tests (RS0T5, RS0T23 and RS0T50) were conducted on saturated recompacted loess at different temperatures of 5, 23 and 50°C). Similarly, another three tests (RS100T5, RS100T23 and RS100T50) were carried out on recompacted loess at suction of 100 kPa at different temperatures (5, 23 and 50°C). The other two tests (IS0T23 and IS100T23) were carried out on intact loess at room temperature (i.e., 23°C), but at different suctions of 0 and 100 kPa. Details of the suction and temperature controlled compression tests are summarized in Table 1.

The second series of tests included six wetting tests with stress and temperature control. Three tests (R50T5, R50T23 and R50T50) were carried out on recompacted loess at confining stress of 50 kPa, but at different temperatures of 5, 23 and 50°C. To study stress effects on wetting-induced collapse of recompacted loess, a test (R110T23) was carried out at confining stress of 110 kPa under room temperature. Similarly, two tests (I50T23 and I110T23) were designed and conducted to investigate stress effects on wetting-induced collapse of intact loess. Details of the suction and temperature controlled wetting tests are summarized in Table 2.

TEST APPARATUS

A suction- and temperature-controlled double cell triaxial apparatus (Ng et al., 2016a) was used in this study. Fig. 1 shows a schematic diagram of this apparatus. The axis translation technique (Hilf, 1956) is adopted to control matric suction ($u_a - u_w$) of soil specimen by adjusting pore-air pressure u_a and pore-water pressure u_w independently. u_a is controlled through a low air-entry value (AEV) porous stone and u_w is controlled through a saturated high AEV (5 bar) ceramic disk. Volumetric strain of soil specimen is measured by using double cell volume change measuring system (Ng et al., 2012), which has an accuracy of 0.03% for the tested specimens (76 mm in diameter and 20 mm in height). The water volume change of the soil specimen is measured by the water flow in and out through a ballast tube connected with an air trap and a burette.

To control soil temperature, a heating/ cooling bath connected with a spiral copper tube installed between the inner cell and outer cell was installed. The heating/ cooling bath consists of a thermostat, a heating/ cooling unit, a water bath, an inbuilt pump and a thermocouple. The thermocouple is installed in the water of the inner cell. The thermostat is used to adjust the output of the heating/cooling unit according to current and target temperatures. Both the thermocouple and the heating/ cooling bath are connected to the thermostat, forming an automatic control and feedback system. In this study, 48 hours are allowed to reach the target temperature and to achieve the thermal equilibrium. After reaching thermal equilibrium, the temperature fluctuation is less than 0.2℃. More details of the temperature control system were

reported by Ng et al. (2016a).

SOIL TYPE AND SPECIMEN PREPARATION

In this study, a loess taken from Shaanxi Province of China is tested. The fractions of sand, silt and clay are 0.1%, 71.9% and 28.0%, respectively. The plastic and liquid limits are 19% and 36%, respectively. The maximum dry density and optimum water content determined from standard Proctor test are 1680 kg/m^3 and 18.1%, respectively. Index properties of this soil are summarized in Table 3. It is classified as a clay of low plasticity (CL) according to the Unified Soil Classification System (ASTM, 2011).

Intact block samples with 300 mm in length of the side were extracted from the depth of 3.5 m. Intact specimens were obtained by using a cutter ring with 76 mm in diameter and 20 mm in height. The initial void ratio is 1.15±0.03. The initial suction and initial water content were 200±20 kPa and 11%, respectively.

For recompacted specimen, the size was also 76 mm in diameter and 20 mm in height. Each specimen is statically compacted in two layers. To be consistent with the intact loess, the compaction water content was about 11% and the initial void ratio is 1.17. After compaction, the initial suction of soil specimen was about 180 kPa.

TEST PROCEDURES

Fig. 2 shows the thermo-hydro-mechanical path of each compression test. Each

compression test consists of suction equalisation stage, thermal equalisation stage and isotropic compression stage. After setting up in the double cell triaxial apparatus, the initial state of intact specimen was fixed at point A (initial suction of 200 kPa) and that of recompacted specimen was controlled at point A' (initial suction of 180 kPa). The suction equalisation stage is to ensure that the water content reaches its equilibrium state throughout soil specimen at the target suction value. For the tests RS100T5, RS100T23, RS100T50 and IS100T23, the soil specimens were wetted to 100 kPa (A→B1, A' →B1). Similarly, for the tests RS0T5, RS0T23, RS0T50 and IS0T23, the soil specimens were wetted to 0 kPa (A→B2, A' →B2). When the water flow rate is less than 0.1 ml/day, the equilibrium state is considered to be reached (Ng et al., 2012). This stage usually takes 7-10 days for achieving the suction equilibrium. Following suction equilibrium, the second stage is for thermal equalisation. Soil specimens in tests RS100T50 and RS0T50 were heated to 50℃ (B1→C3; B2→C1). Similarly, soil specimens in tests RS100T5 and RS0T5 were cooled to 5℃ (B1→C4; B2→C2). For the two tests RS100T23 and RS0T23, the temperatures were kept at room temperature. This stage lasted for 2 days, which was found sufficient to achieve thermal equilibrium based on the readings of thermocouples. The last stage was to isotropically compress all soil specimens to 300 kPa step by step (5-10-20-40-80-150-300 kPa) at drained condition (C1→D1; C2→D3; C3→D4; C4→D6; B1→D5; B2→D2). The detailed stress paths of each compression test are summarized in Table 1.

Fig. 3 shows the thermo-hydro-mechanical path of each wetting test. Each test

178 consists of four stages: isotropic compression, wetting from initial suction to 100
179 kPa, thermal equalisation and wetting from 100 to 0 kPa. Each specimen was first
180 isotropically compressed to a target confining stress at drained condition. The
181 confining stress was 50 kPa for tests R50T5, R50T23 and R50T50 and 110 kPa for
182 tests R110T23 and I110R23. The second stage was to wet all specimens to 100 kPa
183 (B→D1, B'→D1, C→D2, C'→D2). This stage needs 7-10 days for to satisfy the
184 equilibrium criteria that the water flow rate is less than 0.1 ml/day. The following
185 stage was to change soil temperature. Soil temperatures in tests R50T5 and R50T50
186 were changed to 5 and 50℃, respectively (D1→E1, D1→E2). For the other six tests
187 conducted at room temperature, the temperatures were kept constant. Similar to
188 compression tests, two days were allowed for each specimen to achieve thermal
189 equilibrium. The final stage is wetting from 100 to 0 kPa (E1→F3, E2→F4, D1→F1,
190 D2→F2) at constant stress and temperature condition. During the wetting process,
191 soil suction was decreased step by step (100-50-10-1-0 kPa). At each suction, the
192 equilibrium state is reached. The stress paths of all tests are summarized in Table 2.
193

194 **INTERPRETATIONS OF EXPERIMENTAL RESULTS**

195 *Thermal effects on yielding behaviour of recompacted loess*

196 Fig. 4 shows thermal effects on isotropic compression behaviour of recompacted
197 loess. As expected, with increasing confining stress, the void ratio of each specimen
198 decreases. Each compression curve clearly has two approximately linear segments.
199 The pressure at the intersection of these two linear segments is defined as yield stress

200 (Sridharan et al., 1991). The determined yield stresses at different suctions and
201 temperatures are also shown in the figure. At suction of 0 kPa, the yield stresses are
202 about 13, 10 and 7 kPa at 5, 23 and 50℃, respectively. At suction of 100 kPa, the
203 yield stresses are about 42, 40 and 38 kPa at 5, 23 and 50℃, respectively. Effects of
204 suction and temperature on yield stress are further discussed later by analysing the
205 stabilization effects of meniscus water on soil skeleton (Fisher, 1926).

206 In addition, soil compressibility at various suctions and temperatures can be
207 deduced from the compression behaviour shown in Fig. 4. The values of plastic
208 compressibility index λ, which equals to the slope of the second linear segment of
209 each curve, are 0.12 and 0.15 at suctions of 0 and 100 kPa, respectively. At a higher
210 suction, the plastic compressibility index λ becomes slightly larger. On the other
211 hand, thermal effects on λ are not obvious at each suction condition. The observed
212 thermal effects on compressibility in this study keeps consistent with previous
213 experimental results (Cekerevac and Laloui, 2004; Abuel-Naga et al., 2007; Tang et
214 al., 2008; Di Donna and Laloui, 2015).

215 Fig. 5 shows thermal effects on the loading collapse characteristics, which
216 represents the relationship between suction and yield stress, of recompacted loess.
217 The yield stresses at various suctions and temperatures are obtained from Fig. 4. It
218 can be seen that, at a given temperature, the yield stress increases significantly with
219 increasing suction. This is because an increase in suction induces more meniscus
220 water, which provides additional stabilizing effects on soil skeleton and minimize
221 particle rearrangements (Wheeler et al., 2003). The stabilizing effects can be

described by suction-dependent inter-particle normal force ΔN. Assuming that contact angle is zero, ΔN between two spherical particles with the same radius can be expressed by the following analytical solution proposed by Fisher (1926):

$$\Delta N = \frac{\pi {T_s}^2}{s} \frac{\left(\sqrt{9+\frac{8Rs}{T_s}}-3\right)\left(\sqrt{9+\frac{8Rs}{T_s}}+1\right)}{4} \quad (1)$$

where T_s is the surface tension coefficient of water; s is matric suction of soil; and R is the radius of spherical particles. Both T_s and R can be considered as constant at an isothermal condition. It should be noted that equation (1) is a theoretical idealization, without considerations of complex shapes and arrangements of soil particles. This equation can be used to deduce general trends, but not to quantify thermal and suction effects on capillary forces. According to equation (1), ΔN increases with increasing suction, suggesting that stabilizing effects of suction become more significant with increasing suction (Gallipoli et al., 2003; Wheeler et al., 2003; Zhou et al., 2015b). Consequently, yield stress of unsaturated soil increases with increasing suction. The observed reduction of yield stress with decreasing suction is applicable at relatively low suction. At extremely high suctions with a degree of saturation below about 30%, the loss of water meniscus during drying would cause a reduction of suction-induced stabilizing effects (Wan et al., 2014).

It can be also seen from the figure that yield stress at a given suction decreases with increasing temperature (thermal softening). This may be explained by thermal effects on T_s and R in equation (1). According to Gittens (1969), surface tension T_s decreases with increasing temperature. For example, when temperature increases from 23 to 50°C, T_s decreases from 72.3 to 67.9 mN/m. At 5°C, T_s is 74.9 mN/m.

244 The variation of R can be estimated by using the thermal expansion coefficient of
245 soil particles. According to Horseman and McEwen (1996), for clay particles, the
246 thermal expansion coefficient is about 2.9×10^{-3}%/°C. Taking into account of thermal
247 effects on T_s and R, when temperature increases from 23 to 50°C, ΔN decreases
248 by 6.0% and 5.6% at suctions of 0 and 100 kPa, respectively. Similarly, when
249 temperature decreases from 23 to 5°C, ΔN increases by 3.4% and 2.1% at suctions
250 of 0 and 100 kPa, respectively. ΔN decreases with increasing temperature, suggesting
251 that stabilizing effects of suction become less significant with increasing temperature
252 (Ng and Zhou, 2014). Thus, with increasing temperature, the yield stress at a given
253 suction decreases.
254
255 *Comparison between the yielding characteristics of recompacted and intact loess*
256 Fig. 6 shows the isotropic compression behaviour of recompacted and intact
257 loess at suctions of 0 and 100 kPa at 23°C. At zero suction, the yield stress of
258 recompacted specimen is around 10 kPa. When suction increases to 100 kPa, the
259 yield stress of recompacted specimen is 4 times as large as that at zero suction (40
260 kPa). For intact loess, the yield stress is about 25 kPa at suction of 0 kPa. When the
261 suction becomes 100 kPa, the yield stress of intact specimen is 90 kPa, which is 2.6
262 times larger than that at zero suction.
263 As expected, at zero suction, the yield stress of intact specimen is 1.5 times
264 larger than that of recompacted one. At suction of 100 kPa, the yield stress of intact
265 specimen is 1.3 times larger than that of recompacted one. The difference between

recompacted and intact specimens is mainly attributed to more resistant soil fabric of intact specimen than recompacted one (Burland, 1990). As evidenced by microstructural observations (Ng et al., 2016b), there are more clay aggregates accumulated at inter-particle contacts in intact loess compared with recompacted one. The enlargement of contact area minimizes slippages at silt contacts and stiffens the soil skeleton.

The plastic compressibility indices λ of recompacted soil specimens at suctions of 0 and 100 kPa are 0.12 and 0.15, respectively. For intact soil specimens, the plastic compressibility indices λ are 0.13 and 0.17 at suctions of 0 and 100 kPa. The larger λ of intact specimens may be because different from recompacted loess, there are some extra-large pores with a diameter over 200 μm in intact loess (Bai et al., 2014; Ng et al., 2016a). These extra-large pores collapse easily under compression, inducing a larger compressibility for intact loess.

Fig. 7 compares the loading collapse characteristics of recompacted and intact loess at 23°C. The data points in this figure are yield stresses obtained from Fig. 6. As expected, wetting-induced softening is observed in both recompacted and intact loess specimens. Wetting-induced softening of intact loess is more significant than that of recompacted one. This is likely because there are more clay aggregates accumulated at inter-particle contacts in intact specimens, evidenced by microstructural observations and discussed above. The clay aggregates accumulated at inter-particle contacts can provide stronger support to soil skeleton at unsaturated state, with the contributions of capillary force (Barden et al., 1973; Li et al., 2016).

As a result, wetting-induced softening of intact loess specimen is larger than that of recompacted one.

Thermal effects on wetting-induced collapse of recompacted loess

Fig. 8 shows thermal effects on wetting-induced collapse of recompacted loess during wetting from 100 to 0 kPa. The volumetric strain ε_v during this process is calculated using the following equation:

$$\varepsilon_v = -\frac{e_{100}-e_i}{1+e_{100}} \quad (2)$$

where e_{100} is the void ratio at suction of 100 kPa; e_i is the void ratio at a given suction value during the wetting process. Before wetting from 100 to 0 kPa, contractive volumetric strains of about 9% have been observed in the three specimens during the process of compression to 50 kPa and wetting from initial suction to 100 kPa. It is reasonable to assume that all the three specimens are normally consolidated at the stress state with suction of 100 kPa and confining stress of 50 kPa.

It can be seen from the figure that, with decreasing suction, the wetting-induced volumetric strain of recompacted loess increases, at an increasing rate. Moreover, with increasing temperature, the cumulative collapse strain increases. When wetting to 0 kPa, the cumulative collapse volumetric strain at 5℃ is about 4%, which is 20% less than that at room temperature (about 5%). The collapse volumetric strain at 50℃ is around 12%, which is three times of that at 5℃. The thermal effects on wetting-induced collapse can be explained using the yielding characteristics reported

in Fig. 5. As can be seen from Fig. 5, the wetting-induced softening becomes more significant with increasing temperature. The coupled effects of suction and temperature on yield stress can be explained using equation (1). When suction decreases from 100 to 0 kPa, ΔN decreases by about 8.4%, 9.9% and 10.3% at 5, 23 and 50°C, respectively. With a larger reduction of the stabilizing inter-particle normal force at a higher temperature, the wetting-induced softening becomes larger at 50°C than at 5°C.

According to elasto-plastic model for unsaturated soil (e.g. Alonso et al., 1990), there is a positive relationship between incremental volumetric strain $d\varepsilon_v$ and incremental yield stress:

$$\mathrm{d}\varepsilon_{\mathrm{v}} = \frac{\lambda(0)}{1+\mathrm{e}} \frac{\mathrm{dp}_{\mathrm{c}}^{0}}{\mathrm{p}_{\mathrm{c}}^{0}} \tag{3}$$

where $\lambda(0)$ is the plastic compressibility index at zero suction; e is void ratio; p_c^0 is the initial yield stress at zero suction and dp_c^0 is the incremental yield stress at zero suction. To determine the values of p_c^0 and dp_c^0 in equation (3), the yield stress of recompacted loess before and after wetting are shown in Fig. 9. As discussed above, the soil specimens at different temperatures are all normally consolidated before wetting from 100 to 0 kPa. The stress states of each specimen should be located on the corresponding loading collapse (LC) curves. In the current study, it is assumed that the shape of loading collapse curve remains the same before and after wetting. This assumption is supported by the experimental results of Nowamooz and Masrouri (2008) on a bentonite/silt mixture. It was found that the loading collapse curves are almost parallel in a similar suction range (0 to 100 kPa) as that in current study. Under

this assumption, the LC curves before wetting from 100 to 0 kPa are obtained by parallelly shifting those shown in Fig. 5. During the following wetting process, all the three LC curves at different temperatures shift to the right. After wetting to 0 kPa, the stress state at each stress and temperature condition is on the corresponding LC curves. Then, the ratio dp_c^0/p_c^0 can be obtained. As can be seen from Fig. 9, dp_c^0/p_c^0 induced by the wetting process increases with increasing temperature. Consequently, based on equation (3), the wetting-induced yielding and volumetric contraction are larger at a higher temperature, as shown in Fig. 8. This observation implies that at a higher temperature, wetting-induced soil contraction and ground movement would be much larger. Through a series of stress-controlled wetting tests at room temperature, Sun et al. (2007) found that wetting-induced collapse strain is more sensitive to variations in the degree of saturation than variations in the suction. The degrees of saturation of each specimen before and after wetting from 100 to 0 kPa are listed in Table 2. It can be found that the incremental degree of saturation and collapse volumetric strains of the tested loess are consistently larger at a higher temperature. This result suggests that the finding of Sun et al. is applicable to different temperatures.

Comparisons between wetting-induced collapse of recompacted and intact loess

Fig. 10 shows the volumetric collapse of recompacted and intact during wetting from 100 to 0 kPa at various stresses and at 23°C. The volumetric strain ε_v during

this wetting process is also calculated using equation (2). For the recompacted loess specimens, there are 9% and 12% volumetric strain have been observed at confining stress of 50 and 100 kPa at previous compression and wetting stages, respectively. The recompacted specimens can be regarded as normally consolidated prior to wetting from 100 to 0 kPa. The intact specimen at confining stress of 110 kPa shows similar behaviour to recompacted specimens. Before wetting from 100 to 0 kPa, the specimen can be assumed as normally consolidated. On the contrary, the intact loess specimen at stress of 50 kPa shows almost zero volumetric strain at previous compression and wetting stages. This implies that this intact specimen can be regarded as overly consolidated before wetting from 100 to 0 kPa.

It can be found from the figure that for recompacted specimens, when confining stress increases from 50 to 110 kPa, the volumetric strain induced by wetting from 100 to 0 kPa decreases from around 5.5% to 2.4%. On the contrary, in the same confining stress range, the wetting-induced volumetric strain of intact specimen increases from about 1.6% to 3.5%. Furthermore, at confining stress of 50 kPa, the wetting-induced volumetric strain of recompacted specimen is about 3.4 times as large as that of intact one. At confining stress of 110 kPa, the wetting-induced volumetric strain of recompacted specimen is 30% less than that of intact one.

The wetting-induced collapse of recompacted and intact loess can be explained using the measured yielding characteristics shown in Fig. 7. Fig. 11(a) shows the change of yield stress of recompacted specimens before and after wetting from 100 to 0 kPa at different stresses. As discussed above, the recompacted specimen at

376 confining stress of 50 and 110 kPa are normally consolidated before wetting from
377 100 to 0 kPa. The stress states are on the corresponding LC curves. Thus, the LC
378 curves before wetting from 100 to 0 kPa are obtained by shifting the initial LC curve
379 of recompacted specimen shown in Fig. 7. During the following wetting process, the
380 LC curve keeps shifting to the right-hand side. After wetting to 0 kPa, soil stress
381 states are on the corresponding shifted LC curves at both stresses of 50 and 110 kPa.
382 Based on the initial and final LC curves, the value of dp_c^0/p_c^0 is deduced and shown
383 in the figure. It is clear that dp_c^0/p_c^0 in equation (3) is larger at a smaller stress.
384 Hence, the wetting-induced yielding and volumetric contraction decreases with
385 increasing stress in the confining stress range, as shown in Fig. 10.

386 Fig. 11(b) shows the change of yield stress of intact specimens before and after
387 wetting from 100 to 0 kPa at different stresses. The collapse volumetric strain of
388 each specimen, induced by wetting from suction of 100 to 0 kPa, is calculated using
389 equation (3) and summarized in Table 2. For recompacted loess, this equation
390 underestimates wetting-induced strain by 57% and 63% at confining stress of 50 and
391 110 kPa, respectively. For intact loess, the wetting-induced strain is overestimated by
392 22% at confining stress of 50 kPa, but underestimated by 20% at confining stress of
393 110 kPa. The discrepancy is likely because this equation predicts soil volume
394 changes based on initial and final conditions of suction and stress only, but it ignores
395 the influence of stress, suction history and path, and the degree of saturation (Alonso
396 et al., 1990; Ng and Xu, 2002; Sun et al., 2007). During the following wetting
397 process, the LC curve is touched and shift to the right. The intact specimen at

confining stress of 110 kPa is similar to the two recompacted specimens, as illustrated in Fig. 11(a). Before and after wetting from 100 to 0 kPa, the stress states are both on the LC curve. As can be seen from the figure, dp_c^0/p_c^0 at confining stress of 110 kPa is larger than that at confining stress of 50 kPa. Based on equation (3), it can be found that the wetting-induced yielding and volumetric contraction of intact specimen increases with increasing confining stress, as shown in Fig. 10.

The collapse volumetric strain of each specimen, induced by wetting from 100 to 0 kPa, is calculated using equation (3) and summarized in Table 2. For recompacted loess, this equation underestimates wetting-induced strain by 57% and 63% at confining stress of 50 and 110 kPa. For intact loess, the wetting-induced strain is overestimated by 22% at confining stress of 50 kPa, but underestimated by 20% at confining stress of 110 kPa. The discrepancy is likely because this equation predicts soil volume changes based on initial and final conditions of suction and stress only, but ignores the influence of stress and suction path and degree of saturation (Alonso et al., 1990; Sun et al., 2007).

On the other hand, at confining stress of 50 kPa, recompacted loess specimen is normally consolidated and intact one is overly consolidated. Hence, recompacted loess has a larger dp_c^0/p_c^0 than intact loess at stress of 50 kPa, resulting in a larger wetting-induced collapse in recompacted loess. The initial void ratios of intact and recompacted specimens are about 1.13±0.02 and 1.17, respectively. The maximum difference in the initial void ratio between the intact and recompacted specimens is about 4%. The influence of initial void ratio on wetting-induced collapse was

investigated by some previous researchers (Sun et al., 2007; Kholghifard et al., 2012) on Pearl clay and silty clay, which are also classified as clay of low plasticity (same as loess). Based on their experimental results, when void ratio increases by 4%, the wetting-induced collapse volumetric strain increases by 10% to 20% in the stress range of 0 to 100 kPa. This 10% to 20% increase of wetting-induced collapse volumetric strain is almost negligible, considering that the collapse volumetric strain of recompacted loess is about 2.5 times larger than that of intact specimen. Hence, it is reasonable to expect that the difference in initial void ratios would not affect any key conclusion drawn in this study. At confining stress of 110 kPa, both recompacted and intact loess specimens are normally consolidated. Due to larger wetting-induced softening of intact specimen than recompacted one (see Fig. 7), dp_c^0/p_c^0 of intact specimen is larger than that of recompacted one during the wetting process. Consequently, the wetting-induced yielding and volumetric contraction of normally consolidated intact specimen is more significant than that of normally consolidated recompacted one.

Moreover, according to the degrees of saturation listed in Table 2, it is found that a larger increment of degree of saturation does not always induce a higher collapse strains when comparing intact and recompacted loess specimens. It seems that the finding of Sun et al. cannot be generalized for both intact and recompacted loess specimens, likely because the influence of degree of saturation is much less significant compared with structure effects. In addition, the degrees of saturation of each specimen before and after wetting from 100 to 0 kPa listed in Table 2 can also be

used to interpret the experimental results using effective stress analysis.

CONCLUSIONS

Yield stress of loess decreases significantly with decreasing suction (wetting-induced softening), because stabilizing inter-particle normal force reduces during wetting. Moreover, the wetting-induced softening of recompacted loess become larger at a higher temperature. The thermal effects are likely because with a given suction reduction, reduction of the stabilizing inter-particle normal force is larger at a higher temperature. In addition, the wetting-induced softening of intact loess is more significant than that of recompacted one.

Under wetting from 100 to 0 kPa at a confining stress of 50 kPa, the wetting-induced volumetric strain of recompacted loess increases from 4.1% at 5°C to 11.7% at 50°C. This is mainly because the wetting-induced softening is larger at a higher temperature, resulting in more significant yielding and volumetric collapse during wetting. This observation implies that at a higher temperature, wetting-induced soil contraction and ground movement would be much larger.

When confining stress increases from 50 to 110 kPa, the wetting-induced volumetric strain of intact specimen increases from about 1.6% to 3.5%. This is because prior to wetting, soil specimen is overly consolidated at 50 kPa but normally consolidated at 110 kPa. On the contrary, the wetting-induced volumetric strain of recompacted specimen decreases from around 5.5% to 1.6% when confining stress increases from 50 to 110 kPa. This is most probably because prior to wetting from 100

464 to 0 kPa, recompacted specimen at both stresses are normally consolidated. Soil
465 specimen at a stress of 110 kPa has a higher density and thus a smaller
466 wetting-induced collapse.

467 At a lower stress of 50 kPa (similar to in situ stress level), wetting-induced
468 softening of intact soil is much smaller than that of recompacted soil. This is because
469 after many drying and wetting cycles in the field, intact soil has a larger yield stress
470 and more resistant structure. At a higher stress of 110 kPa (much higher than in situ
471 stress level), at which both intact and recompacted soils become normally
472 consolidated, wetting-induced volumetric contraction of intact specimen is about 30%
473 larger than that of recompacted specimen. This is mainly because the wetting-induced
474 softening of intact loess is more significant than that of recompacted one.

475

476 **Acknowledgements**

477 The research grants 616812, 16209415 and T22-603/15N provided by the
478 Research Grants Council of the Hong Kong Special Administrative Region (HKSAR)
479 are grateful acknowledged. In addition, the authors would like to thank the National
480 Natural Science Foundation of China for their financial supports from Projects
481 51509041.

482

483 **REFERENCES**

484 Abuel-Naga, H., Bergado, D. T., Bouazza, A. and Ramana, G. V. 2007. Volume
485 change behaviour of saturated clays under drained heating conditions:
486 experimental results and constitutive modelling. Canadian Geotechnical Journal,

487 **44**(8): 942-956.
488 Alonso, E. E., Gens, A. and Josa, A. 1990. Constitutive model for partially saturated
489 soils. Géotechnique, **40**(3): 405–430.
490 ASTM. 2011. Standard practice for classification of soils for engineering purposes
491 (Unified Soil Classification System). ASTM standard D2487. American Society
492 for Testing and Materials, West Conshohocken.
493 Barden, L., McGown, A., and Collins, K. 1973. The collapse mechanism in partly
494 saturated soil. Engineering Geology, **7**(1): 49-60.
495 Bai, X. H., Ma, F. L.,Wang, M. and Jia, J. G. 2014. Micro-structure and collapsibility
496 of loess in China. In Geomechanics from Micro to Macro. *Edited by* K. Soga, K.
497 Kumar, G. Biscontin and M. Kuo. CRC Press, London, UK. pp. 1303–1308.
498 Burland, J. B. 1990. On the compressibility and shear strength of natural clays.
499 Géotechnique, **40**(3): 329-378.
500 Campanella, R. G. and Mitchell, J. K. 1968. Influence of temperature variations on
501 soil behaviour. Journal of Soil Mechanics and Foundations. Div., ASCE, **94**(3):
502 709-734.
503 Cekerevac, C. and Laloui, L. 2004. Experimental study of thermal effects on the
504 mechanical behaviour of a clay. International Journal for Numerical and
505 Analytical Methods in Geomechanics, **28**(3): 209-228.
506 Cui, Y. J. and Delage, P. 1996. Yielding and plastic behaviour of an unsaturated
507 compacted silt. Géotechnique, **46**(2): 291-311.
508 Di Donna, A. and Laloui, L. 2015. Response of soil subjected to thermal cyclic

509 loading: experimental and constitutive study. Engineering Geology, **190**: 65-76.
510 Fisher, R. 1926. On the capillary forces in an ideal soil; correction of formulae given
511 by WB Haines. The Journal of Agricultural Science, **16**(3): 492-505.
512 Gallipoli, D., Gens, A., Sharma, R., and Vaunat, J. 2003. An elasto-plastic model for
513 unsaturated soil incorporating the effects of suction and degree of saturation on
514 mechanical behaviour. Géotechnique, **53**(1): 123-135.
515 Gens, A. 2010. Soil-environment interactions in geotechnical engineering.
516 Géotechnique, **60**(1): 3-74.
517 Gittens, G. J. 1969. Variation of surface tension of water with temperature. Journal
518 of Colloid and Interface Science, **30**(3): 406-412.
519 Haghighi, A., Medero, G., Woodward, P., and Laloui, L. 2011. Effect of temperature
520 on collapse potential of kaolin clay. *In* Unsaturated Soils-Proceedings of the 5th
521 International Conference on Unsaturated Soils, pp. 543-548.
522 Hilf, J. W. 1956. An investigation of pore water pressure in compacted cohesive soils.
523 Technical Memorandum 654, U.S. Bureau of Reclamation, Washington, D.C.
524 Horseman, S. T. and McEwen, T. J. 1996. Thermal constraints on disposal of
525 heat-emitting waste in argillaceous rocks. Engineering Geology, **41**: 5-16.
526 Jiang, M., Hu, H., and Liu, F. 2012. Summary of collapsible behaviour of artificially
527 structured loess in oedometer and triaxial wetting tests. Canadian Geotechnical
528 Journal, **49**(10): 1147-1157.
529 Kholghifard, M., Kholghifard, A., Ahmad, K., and Latifi, N. 2012. The Influence of
530 Suction Changes on Collapsibility and Volume Change Behavior of Unsaturated

Clay Soil. Electronic Journal of Geotechnical Engineering, **17**: 2623-2631.

Lawton, E., Fragaszy, R., and Hardcastle, J. 1989. Collapse of compacted clayey sand. Journal of Geotechnical Engineering, **115**(9): 1252-1267.

Li, P., Vanapalli, S., and Li, T. L. 2016. Review of collapse triggering mechanism of collapsible soils due to wetting. Journal of Rock Mechanics and Geotechnical Engineering, **8**(2): 256-274.

Lloret, A., Villar, M. V., Sanchez, M., Gens, A., Pintado, X. and Alonso, E. E. 2003. Mechanical behaviour of heavily compacted bentonite under high suction changes. Géotechnique, **53**(1): 27–40.

Munoz-Castelblanco, J., Delage, P., Pereira, J. M., and Cui, Y. J. 2011. Some aspects of the compression and collapse behaviour of an unsaturated natural loess. Géotechnique Letters, **1**(2): 17-22.

Ng, C. W. W., Cheng, Q., Zhou, C., and Alonso, E. E. 2016a. Volume changes of an unsaturated clay during heating and cooling. Géotechnique Letters, **6**(3): 192-198.

Ng, C. W. W., Kaewsong, R., Zhou, C., and Alonso, E. E. (2016b). Small strain shear moduli of unsaturated natural and compacted loess [online]. Géotechnique. doi: 10.1680/jgeot.16.T.013

Ng, C. W. W., Lai, C. H., and Chiu, C. F. 2012. A modified triaxial apparatus for measuring the stress path-dependent water retention curve. Geotechnical Testing Journal, **35**(3): 490-495.

Ng, C. W. W., Sadeghi, H., Hossen, S. B., Chiu, C. F., Alonso, E. E., and Baghbanrezvan, S. 2016c. Water retention and volumetric characteristics of intact

553 and re-compacted loess. Canadian Geotechnical Journal, **53**(8): 1258-1269.
554 Ng, C. W. W. and Xu, J. 2012. Effects of current suction ratio and recent suction
555 history on small strain behaviour of an unsaturated soil. Canadian Geotechnical
556 Journal. **49**(2): 226-243.
557 Ng, C. W. W., and Zhou, C. 2014. Cyclic behaviour of an unsaturated silt at various
558 suctions and temperatures. Géotechnique, **64**(9): 709-720.
559 Nowamooz, H., and Masrouri, F. 2008. Hydromechanical behaviour of an expansive
560 bentonite/silt mixture in cyclic suction-controlled drying and wetting tests.
561 Engineering Geology, **101**(3): 154-164.
562 Pereira, J., and Fredlund, D. 2000. Volume change behavior of collapsible
563 compacted gneiss soil. Journal of Geotechnical and Geoenvironmental
564 Engineering, **126**(10): 907-916.
565 Romero, E., Gens, A., and Lloret, A. 2003. Suction effects on a compacted clay
566 under non-isothermal conditions. Géotechnique, **53**(1): 65-81.
567 Sridharan, A., Abraham, B. M., and Jose, B. T. 1991. Improved technique for
568 estimation of yield stress. Géotechnique, **41**(2): 263-268.
569 Sun, D. A., Sheng, D., and Xu, Y. 2007. Collapse behaviour of unsaturated
570 compacted soil with different initial densities. Canadian Geotechnical Journal,
571 **44**(6): 673-686.
572 Tang, A. M., Cui, Y. J. and Barnel, N. 2008. Thermo-mechanical behaviour of a
573 compacted swelling clay. Géotechnique, **58**(1): 45-54.
574 Uchaipichat, A. and Khalili, N. 2009. Experimental investigation of

575 thermo-hydro-mechanical behaviour of an unsaturated silt. Géotechnique, **59**(4):
576 339-353.
577 Villar, M. V. 1999. Investigation of the behaviour of bentonite by means of
578 suction-controlled oedometer tests. Engineering Geology, **54**(1-2): 67-73.
579 Vilar, O. M., and Rodrigues, R. A. 2011. Collapse behavior of soil in a Brazilian
580 region affected by a rising water table. Canadian Geotechnical Journal, **48**(2):
581 226-233.
582 Wan, R., Khosravani, S., and Pouragha, M. 2014. Micromechanical analysis of force
583 transport in wet granular soils. Vadose Zone Journal, **13**(5): 1-12.
584 Wheeler, S. J., Sharma, R. S., and Buisson, M. S. R. 2003. Coupling of hydraulic
585 hysteresis and stress–strain behaviour in unsaturated soils. Géotechnique, **53**(1):
586 41-54.
587 Wheeler, S. J. and Sivakumar, V. 1995. An elasto-plastic critical state framework for
588 unsaturated soils. Géotechnique, **45**(1): 35-53.
589 Zhou, C., Ng, C. W. W., and Chen, R. 2015a. A bounding surface plasticity model for
590 unsaturated soil at small strains. International Journal for Numerical and
591 Analytical Methods in Geomechanics, **39**(11): 1141-1164.
592 Zhou, C., Xu, J. and Ng, C. W. W. 2015b. Effects of temperature and suction on
593 secant shear modulus of unsaturated soil. Géotechnique Letters, **5**(3): 123-128.

List of tables

List of figures

(T = 23°C)

Fig. 11 Evolution of loading collapse characteristics of (a) recompacted loess; (b) intact loess during wetting from 100 to 0 kPa (T = 23°C)

Table 1 Details of suction and temperature controlled compression tests

Test ID	Specimen type	Suction (kPa)	Temperature (°C)	Stress path (See Fig. 2)
a. Thermal effects on compression behaviour of recompacted loess at suction of 0 kPa				
RS0T5	Recompacted	0	5	A'→B2→C2→D3
RS0T23	Recompacted	0	23	A'→B2→D2
RS0T50	Recompacted	0	50	A'→B2→C1→D1
b. Thermal effects on compression behaviour of recompacted loess at suction of 100 kPa				
RS100T5	Recompacted	100	5	A'→B1→C4→D6
RS100T23	Recompacted	100	23	A'→B1→D5
RS100T50	Recompacted	100	50	A'→B1→C3→D4
c. Compression behaviour of intact loess at suctions of 0 and 100 kPa				
IS0T23	Intact	0	23	A→B2→D2
IS100T23	Intact	100	23	A→B1→D5

Table 2 Details of stress and temperature controlled wetting tests

Test ID	Specimen type	p (kPa)	T (°C)	e (initial)	Stress path (See Fig. 3)	ε_v calculated using equation (3) (%)	Sr	
							Before (%)	After (%)
a. Thermal effects on wetting-induced collapse of recompacted loess								
R50T5	Recompacted	50	5	1.17	A'→B'→D1→E1→F3	2.6	46.9	95.2
R50T23	Recompacted	50	23	1.18	A'→B'→D1→F1	2.4	44.9	92.4
R50T50	Recompacted	50	50	1.17	A'→B'→D1→E2→F4	2.3	41.9	90.1
b. Wetting-induced collapse of recompacted loess at varies stresses								
R110T23	Recompacted	110	23	1.17	A'→C'→D2→F2	0.9	49.5	93.6
c. Wetting-induced collapse of intact loess at varies stresses								
I50T23	Intact	50	23	1.12	A→B→D1→F1	2.0	30.4	89.1
I110T23	Intact	110	23	1.13	A→C→D2→F2	2.8	60.0	95.7

Table 3 Index properties of tested loess

Index test	Measured value
Standard compaction tests	
Maximum dry density: kg/m^3	1680
Optimum water content: %	16.3
Grain size distribution	
Percentage of sand: %	0.1
Percentage of silt: %	71.9
Percentage of clay: %	28.0
Specific gravity	2.69
Atterberg limit	
Liquid limit: %	36
Plastic limit: %	19
Plasticity index: %	17

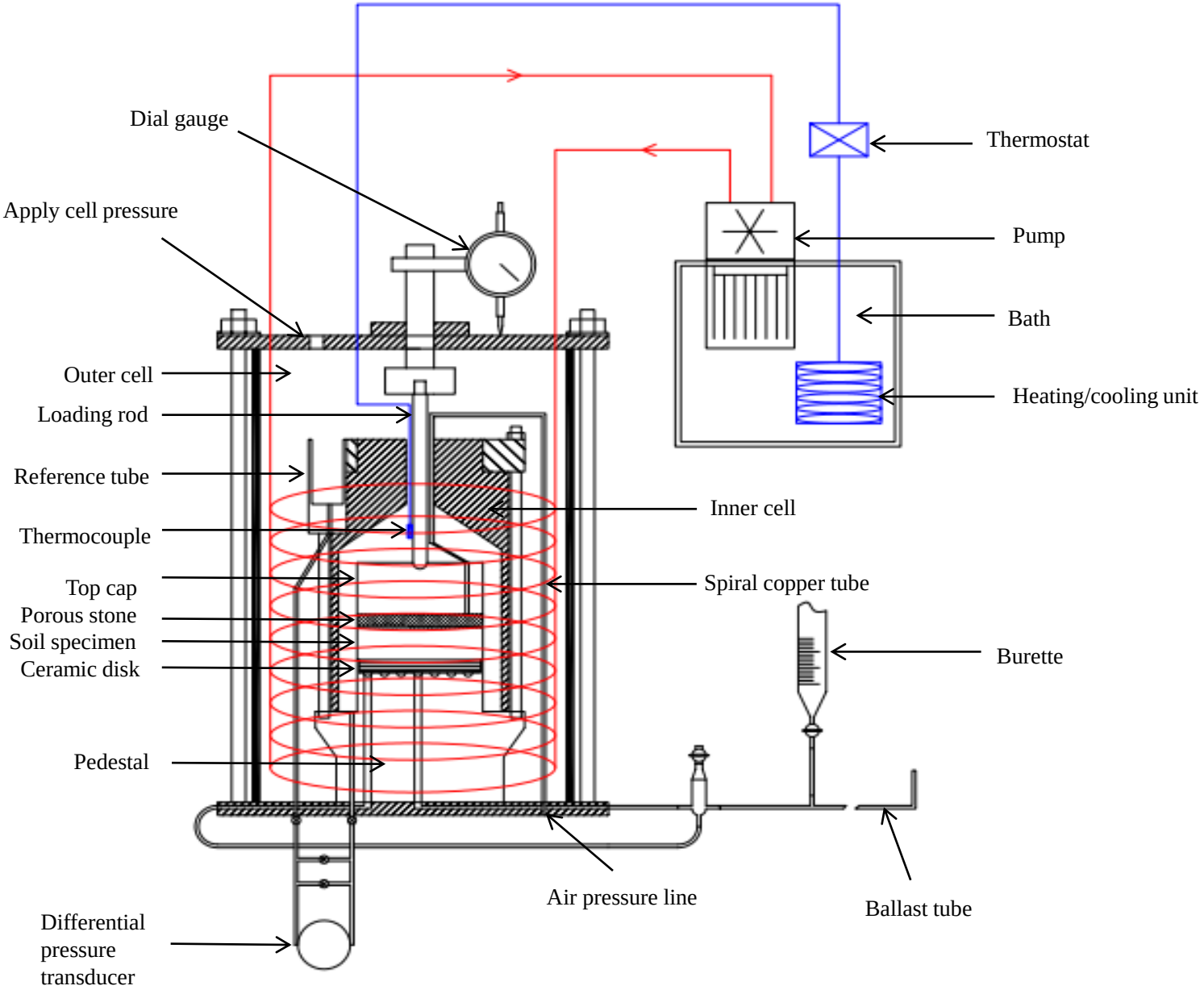
Dial gauge
Apply cell pressure
Outer cell
Loading rod
Reference tube
Thermocouple
Top cap
Porous stone
Soil specimen
Ceramic disk
Pedestal
Differential pressure transducer
Thermostat
Pump
Bath
Heating/cooling unit
Inner cell
Spiral copper tube
Burette
Air pressure line
Ballast tube

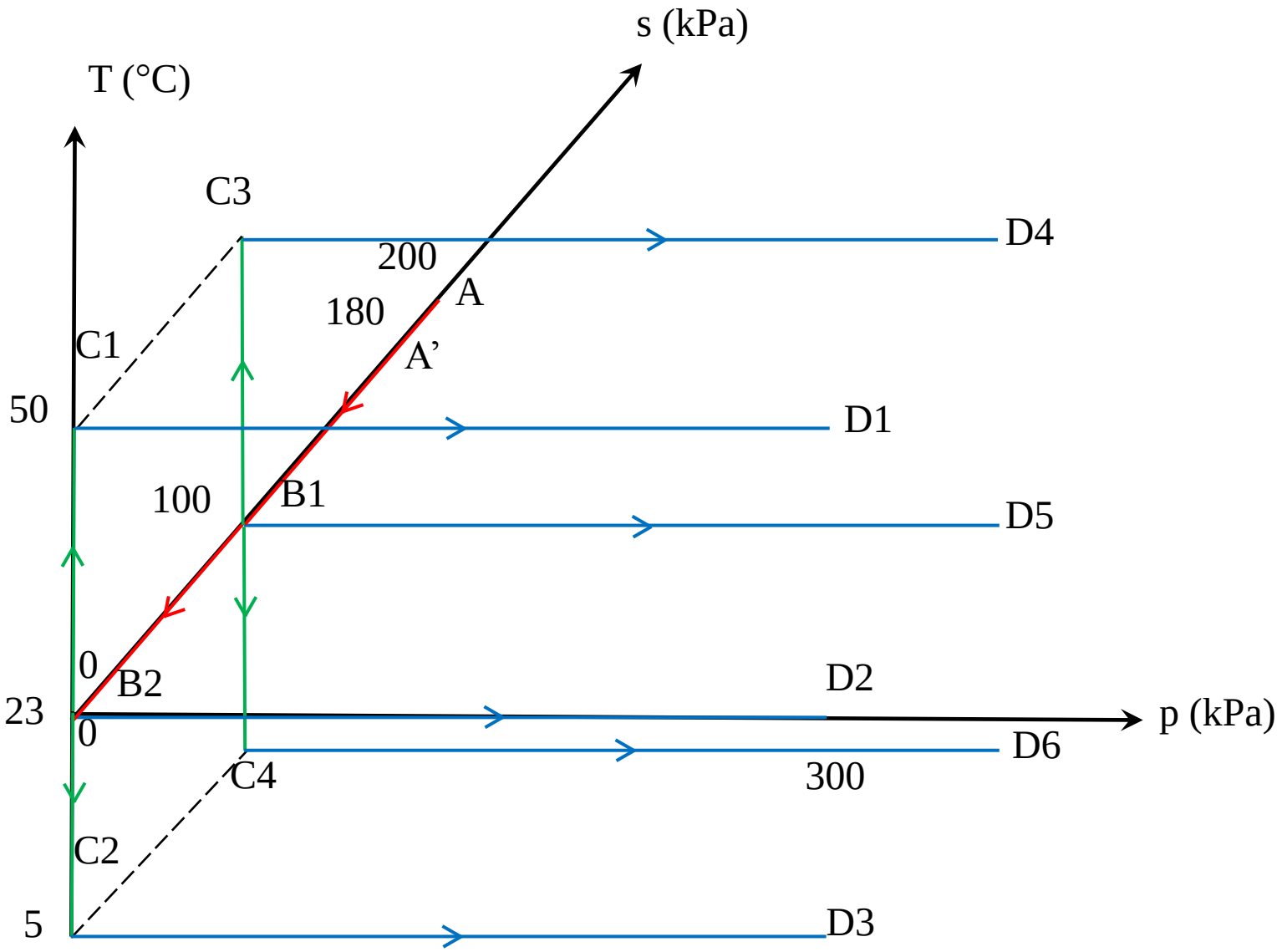
s (kPa)
T (°C)
C3
D4
200
A
180
A'
C1
50
D1
100
B1
D5
0
B2
D2
23
0
p (kPa)
D6
C4
300
C2
5
D3

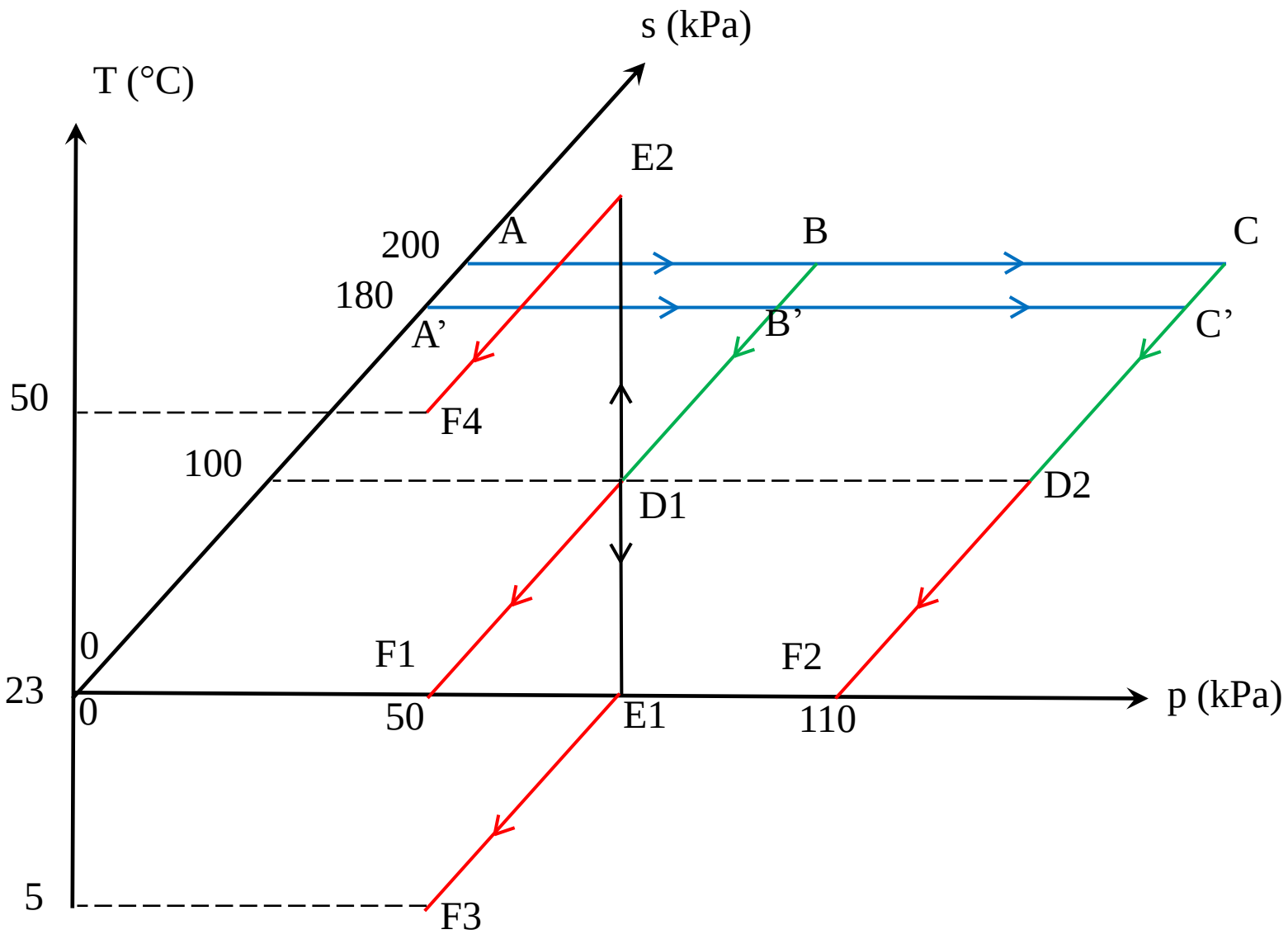
s (kPa)
T (°C)
E2
200
A
B
C
180
A’
B’
C’
50
F4
100
D1
D2
0
F1
F2
23
0
50
E1
110
p (kPa)
5
F3

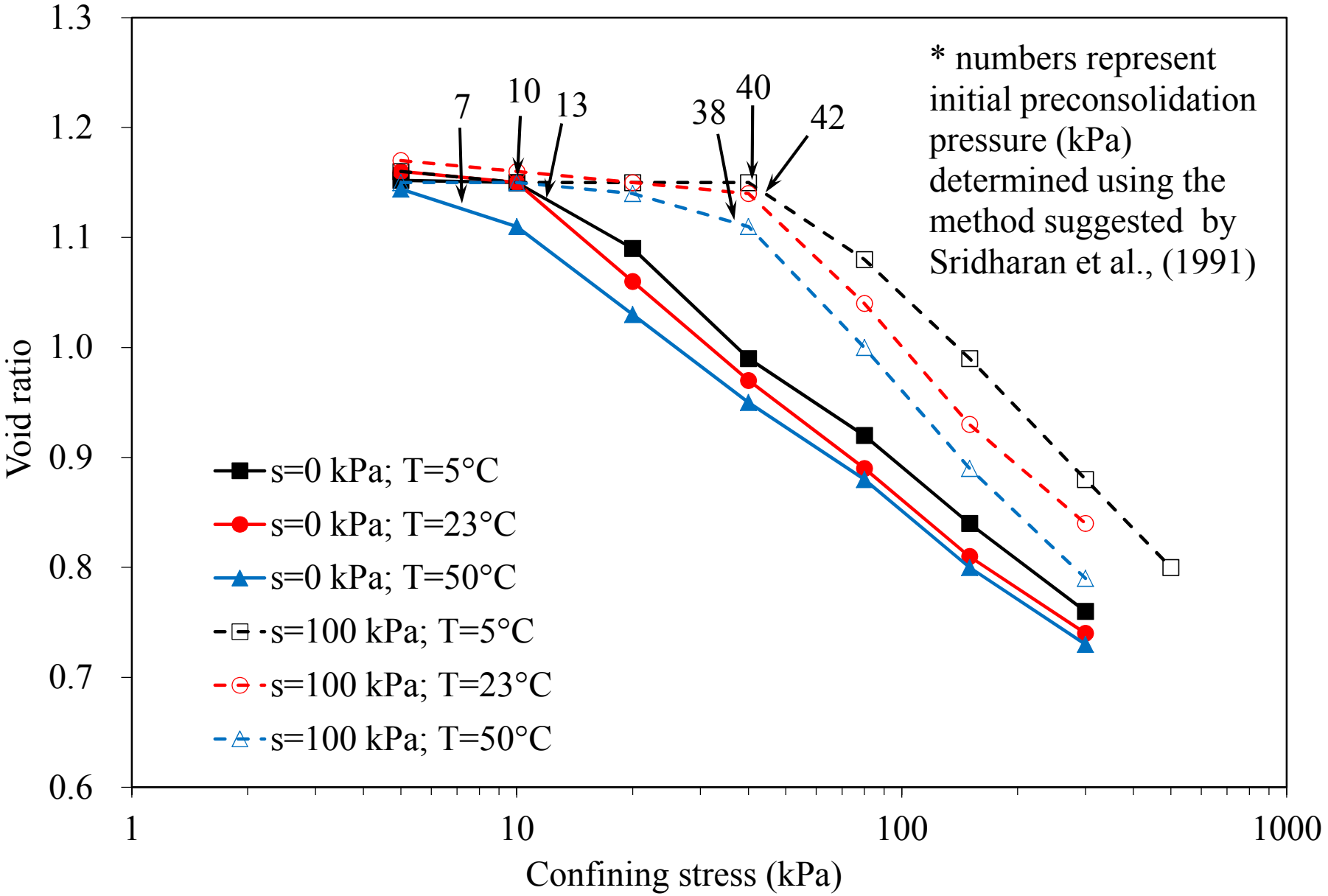
1.3
1.2
1.1
1.0
0.9
0.8
0.7
0.6
Void ratio
1
10
100
1000
Confining stress (kPa)
7
10
13
38
40
42
* numbers represent initial preconsolidation pressure (kPa) determined using the method suggested by Sridharan et al., (1991)
s=0 kPa; T=5°C
s=0 kPa; T=23°C
s=0 kPa; T=50°C
s=100 kPa; T=5°C
s=100 kPa; T=23°C
s=100 kPa; T=50°C

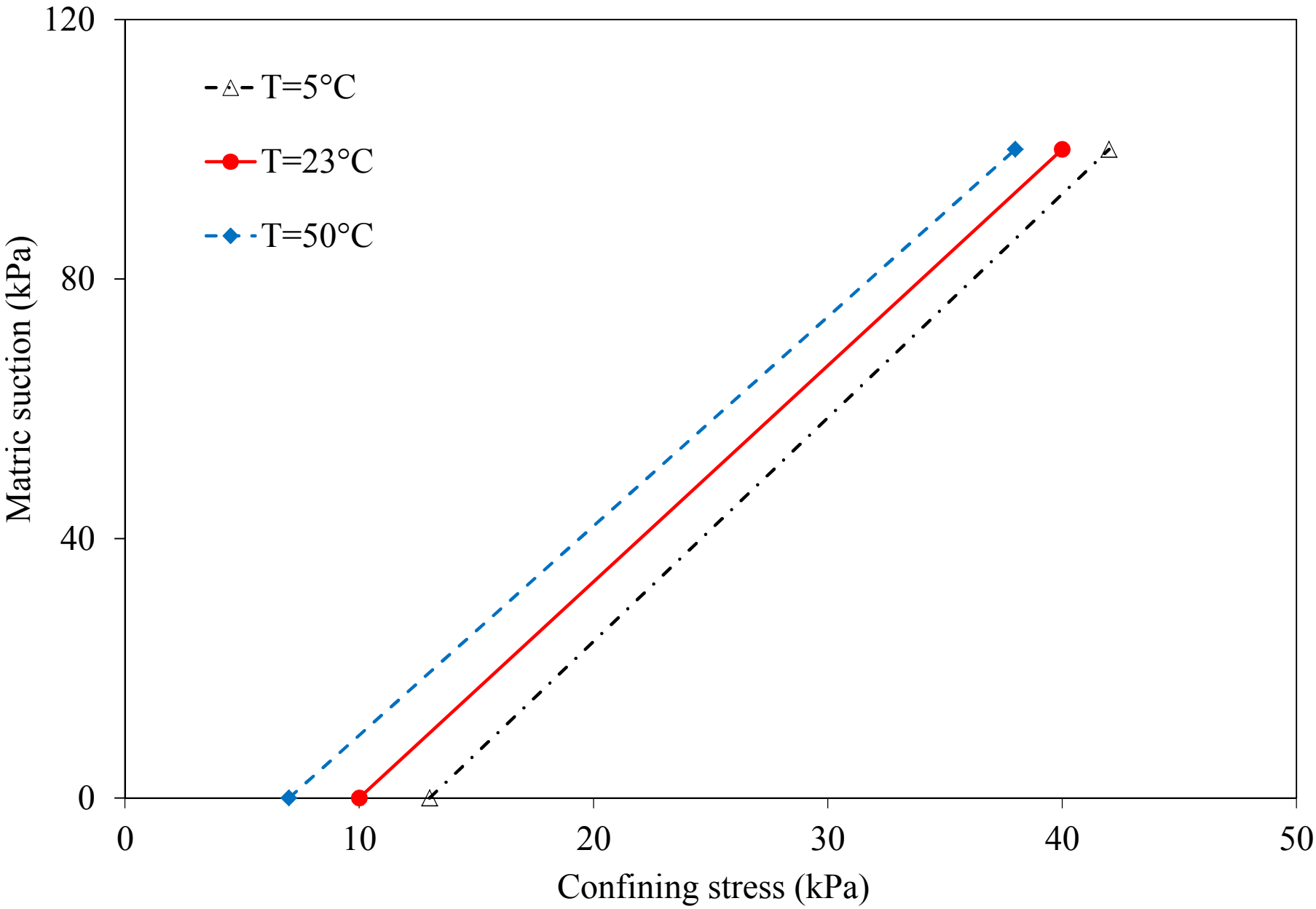
120
80
40
0
Matric suction (kPa)
T=5°C
T=23°C
T=50°C
0
10
20
30
40
50
Confining stress (kPa)

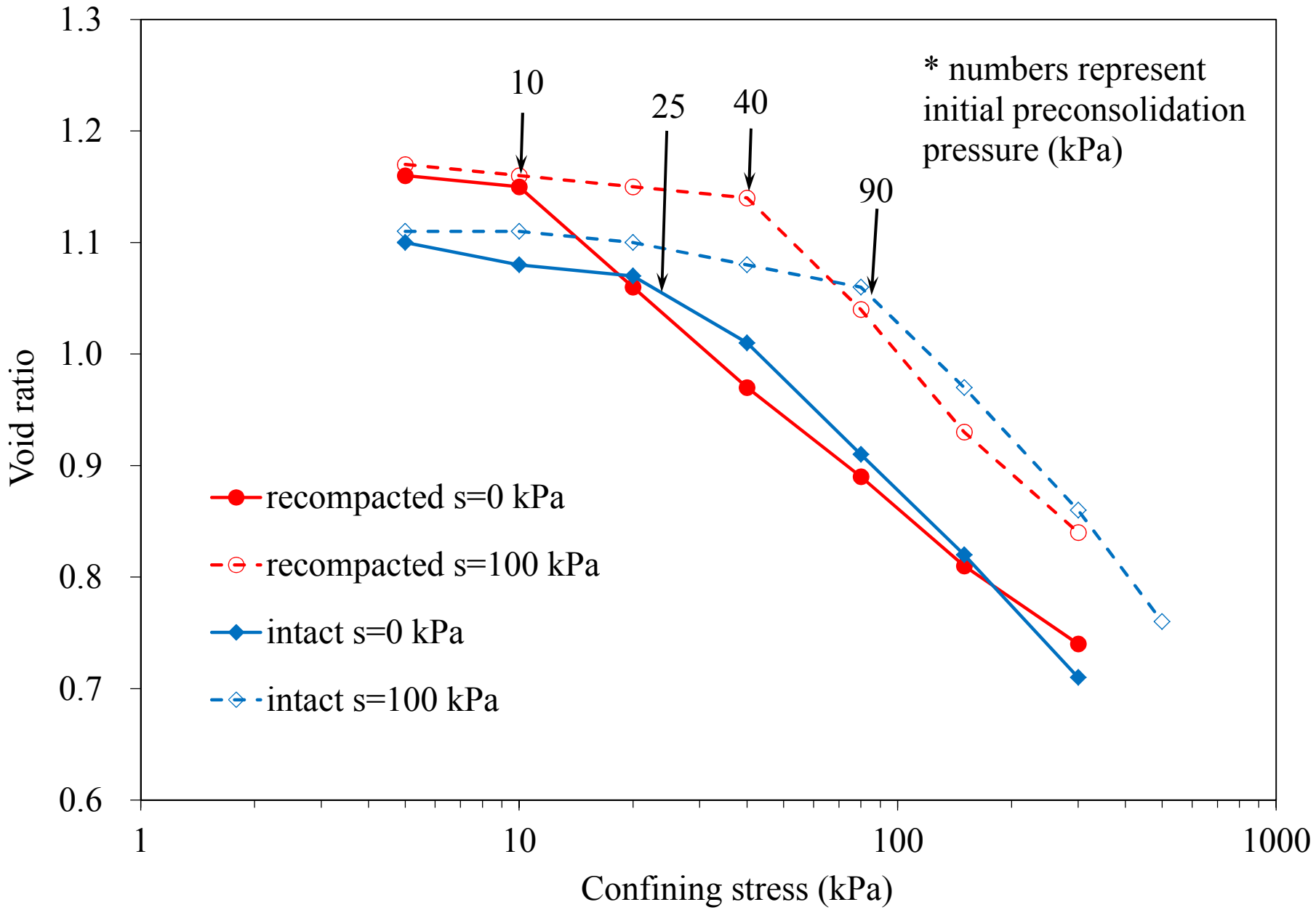
1.3
1.2
1.1
1.0
0.9
0.8
0.7
0.6
Void ratio
1
10
100
1000
Confining stress (kPa)
10
25
40
90
* numbers represent initial preconsolidation pressure (kPa)
recompacted s=0 kPa
recompacted s=100 kPa
intact s=0 kPa
intact s=100 kPa

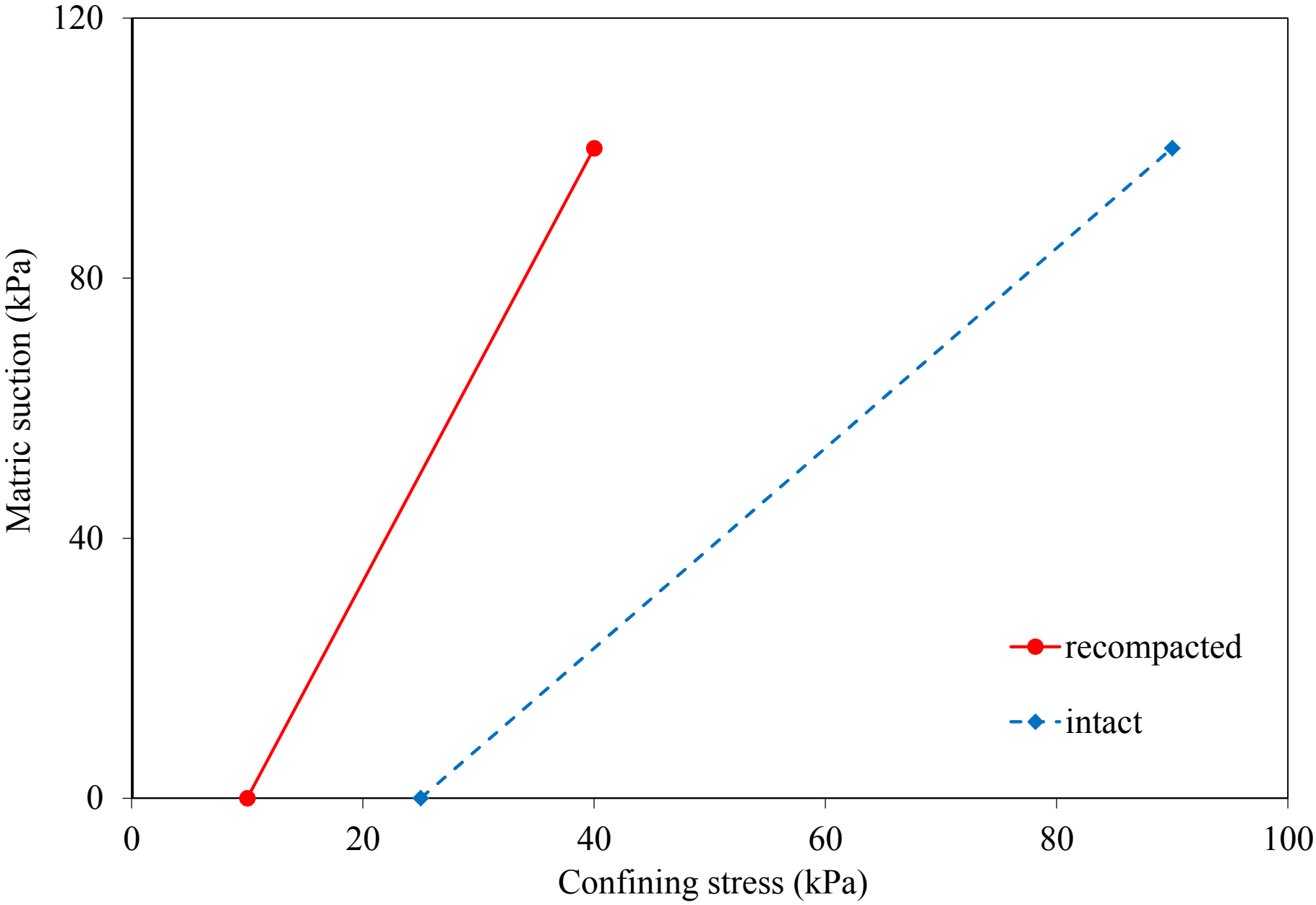
120
80
40
0
Matric suction (kPa)
0
20
40
60
80
100
Confining stress (kPa)
recompacted
intact

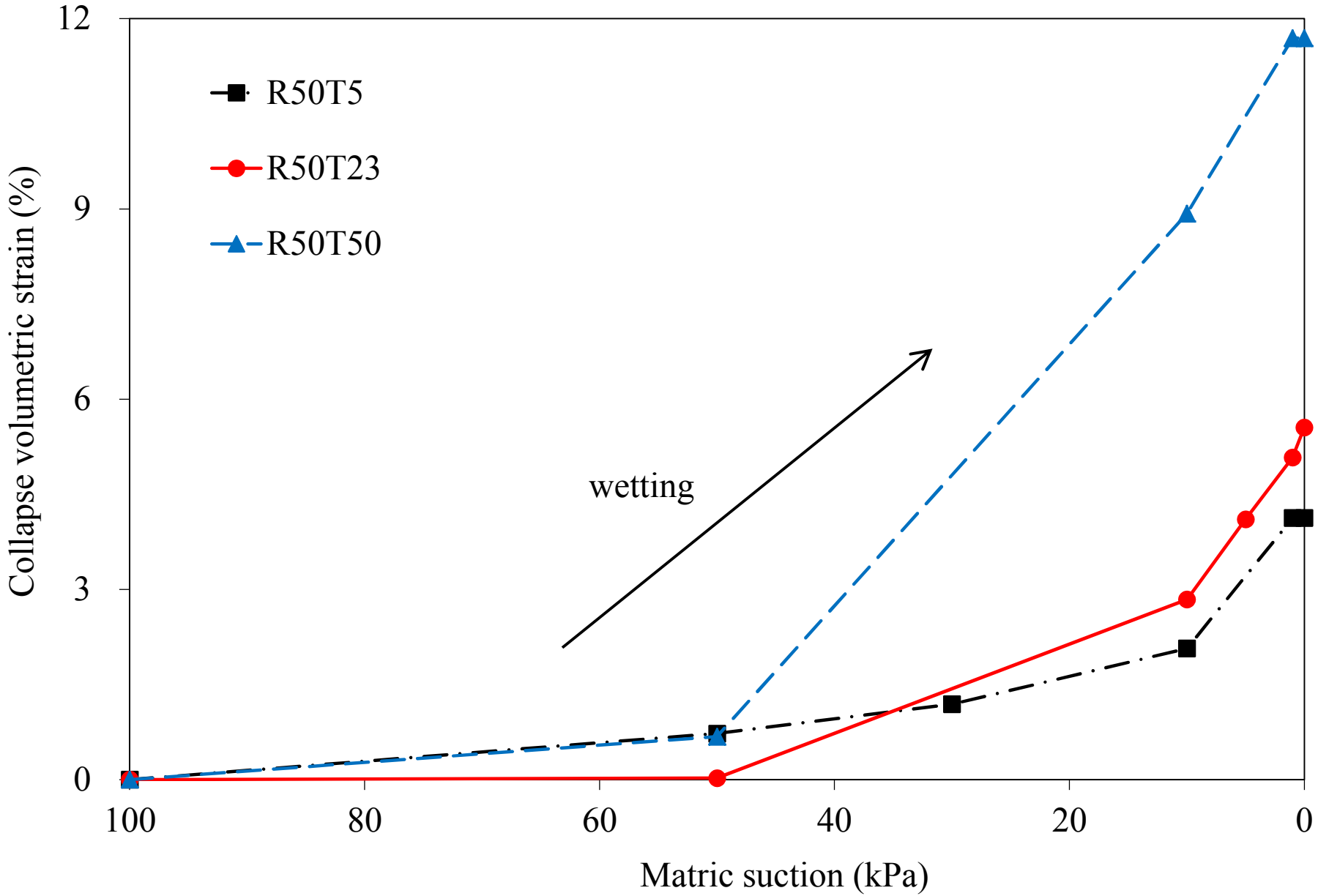
12
9
6
3
0
Collapse volumetric strain (%)
R50T5
R50T23
R50T50
wetting
100
80
60
40
20
0
Matric suction (kPa)

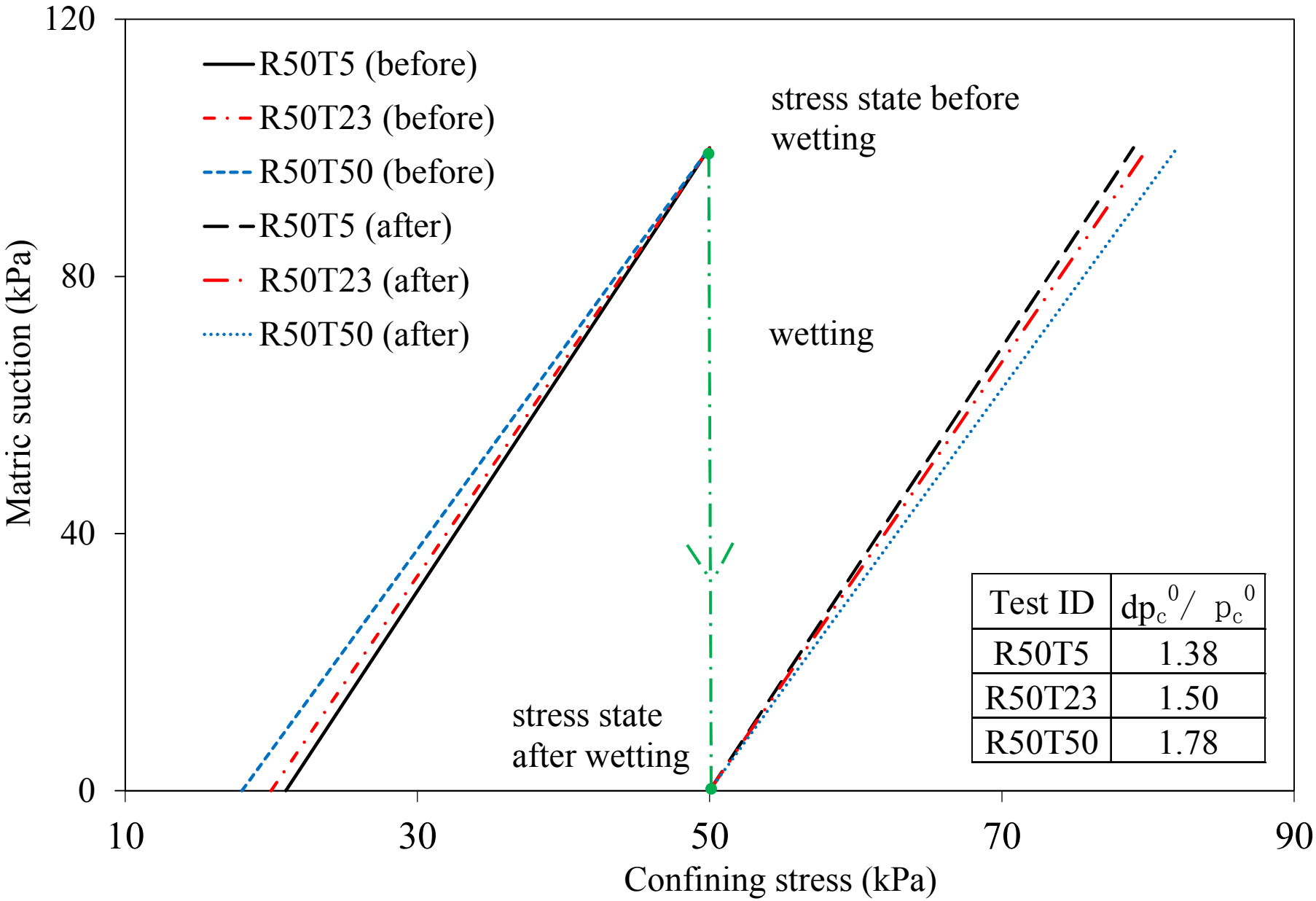
120
80
40
0
Matric suction (kPa)
10
30
50
70
90
Confining stress (kPa)
R50T5 (before)
R50T23 (before)
R50T50 (before)
R50T5 (after)
R50T23 (after)
R50T50 (after)
stress state before wetting
wetting
stress state after wetting
Test ID
dpc0 / pc0
R50T5
1.38
R50T23
1.50
R50T50
1.78

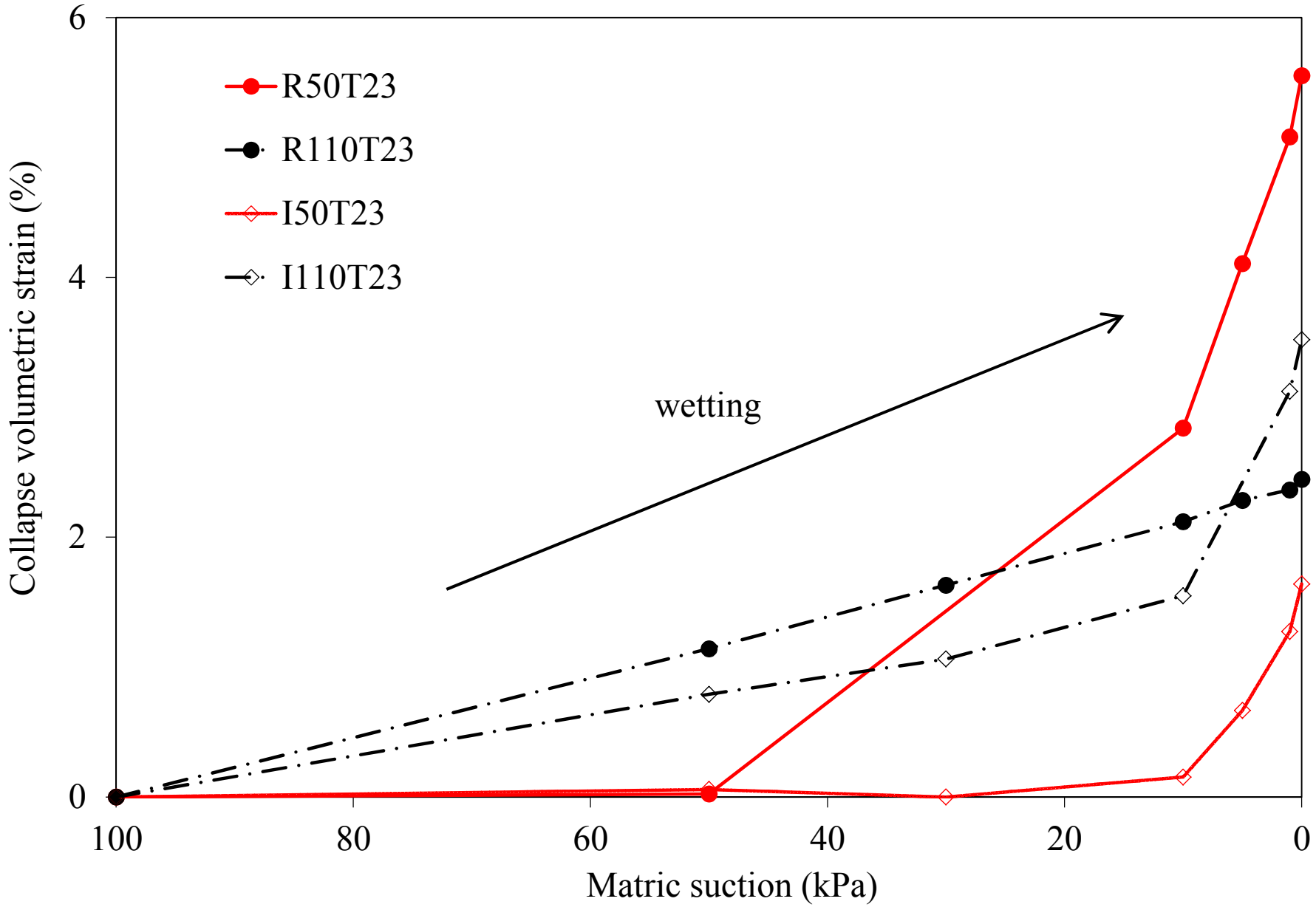
6
4
2
0
Collapse volumetric strain (%)
R50T23
R110T23
I50T23
I110T23
wetting
100
80
60
40
20
0
Matric suction (kPa)

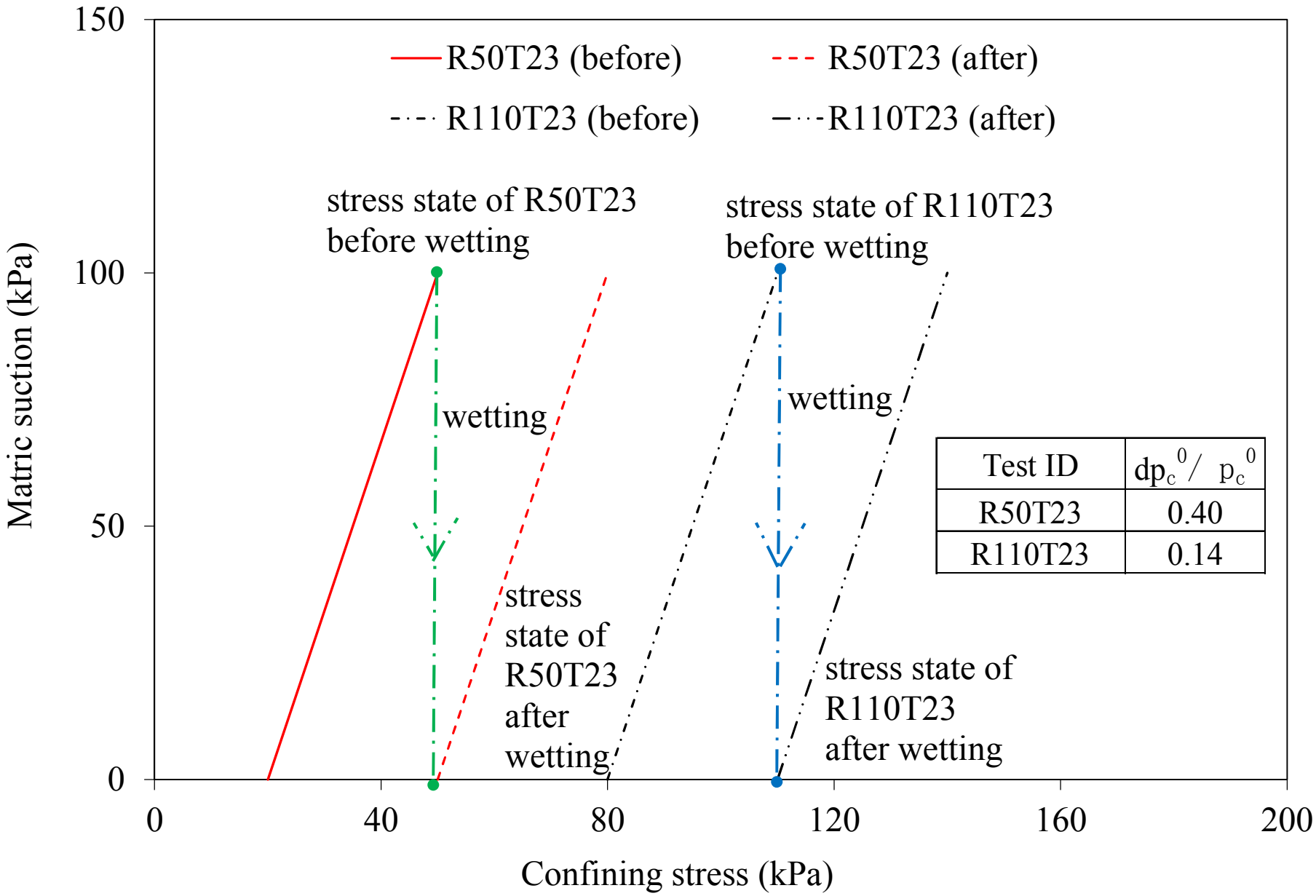
150
100
50
0
Matric suction (kPa)
0
40
80
120
160
200
Confining stress (kPa)
R50T23 (before)
R50T23 (after)
R110T23 (before)
R110T23 (after)
stress state of R50T23 before wetting
stress state of R110T23 before wetting
wetting
wetting
stress state of R50T23 after wetting
stress state of R110T23 after wetting
Test ID
dpc0 / pc0
R50T23
0.40
R110T23
0.14

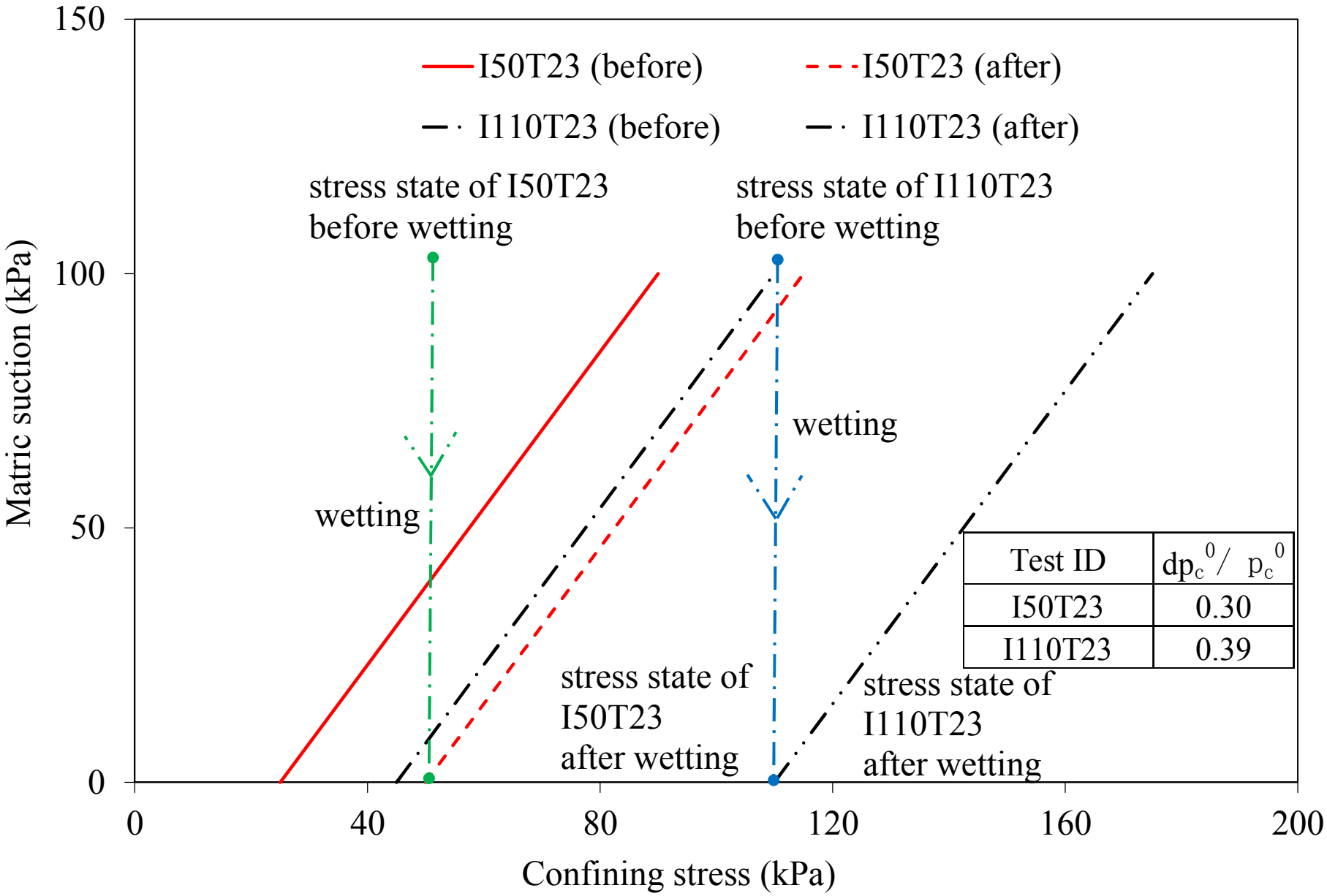
150
100
50
0
Matric suction (kPa)
0
40
80
120
160
200
Confining stress (kPa)
I50T23 (before)
I50T23 (after)
I110T23 (before)
I110T23 (after)
stress state of I50T23 before wetting
stress state of I110T23 before wetting
wetting
wetting
stress state of I50T23 after wetting
stress state of I110T23 after wetting
Test ID
dpc0 / pc0
I50T23
0.30
I110T23
0.39